

This ESI for *J. Mater. Chem. A*, 2019, **7**, DOI: 10.1039/C9TA07361B, originally published on 9th August 2019, was updated on 6th September 2019. An additional figure panel (Fig. S14a) was inserted, which was mistakenly omitted from the published article.

Supporting information

Blade coated P3HT:non-fullerene acceptors solar cells: a high-throughput parameter study with a focus on up-scalability

Enrique Pascual-San-José^{a,b}, Xabier Rodríguez-Martínez^a, Rana Adel-Abdelaleim^{a,b}, Marco Stella^b, Eugenia Martínez-Ferrero^b, Mariano Campoy-Quiles^{*a}

^aInstitut de Ciència de Materials de Barcelona (ICMAB-CSIC), Campus de la UAB, 08193, Bellaterra, Barcelona, Spain;

^bEURECAT, Centre Tecnològic de Catalunya, Parc Científic i de la Innovació TecnoCampus, Av. de Ernest Lluch, 36, 08302, Mataró, Barcelona, Spain;

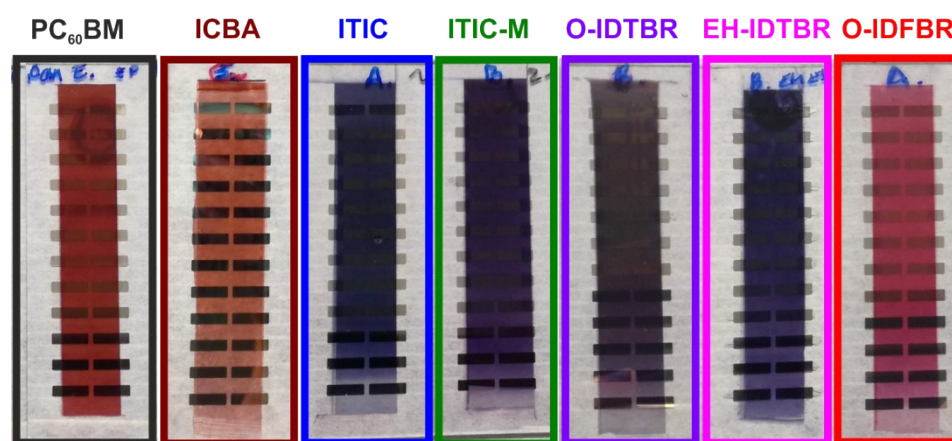


Fig. S1. Picture of thickness gradient samples of P3HT blended with PC₆₀BM, ITIC, ITIC-M, O-IDTBR, EH-IDTBR, O-IDFBR (left to right). Thickness increases from bottom to top.

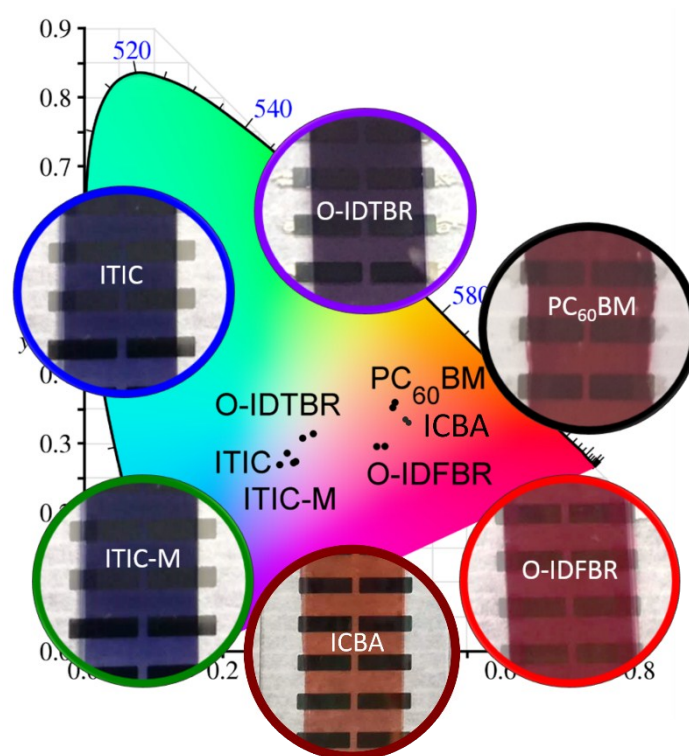


Fig. S2. CIE plot coordinates calculated from transmittance spectra of samples of P3HT blended with PC₆₀BM, ICBA, ITIC, ITIC-M, O-IDTBR, EH-IDTBR, O-IDFBR.

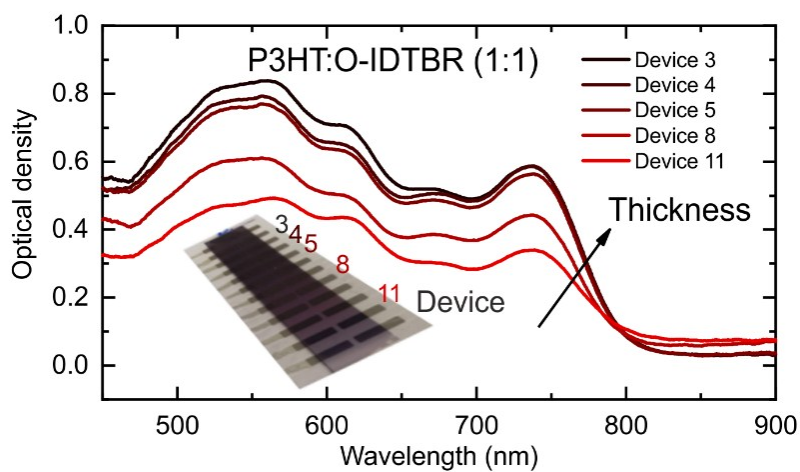


Fig. S3. Optical density of the P3HT:O-IDTBR thickness gradient sample. Inset: Picture of a thickness-gradient sample.

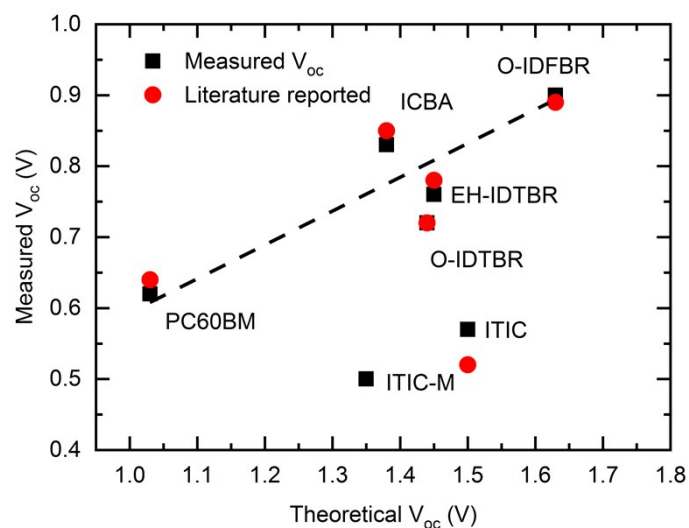


Fig. S4 Measured and theoretical voltage extracted from the energy levels of P3HT based systems for devices reported in this manuscript (black square) and in literature (red circle). P3HT is blended with PC₆₀BM, ICBA, ITIC, ITIC-M, O-IDTBR, EH-IDTBR, O-IDFBR. There is no available data reported for P3HT:ITIC-M system. The energy levels are extracted from literature (references in the manuscript). Dashed line is plotted as a guide to the eye.

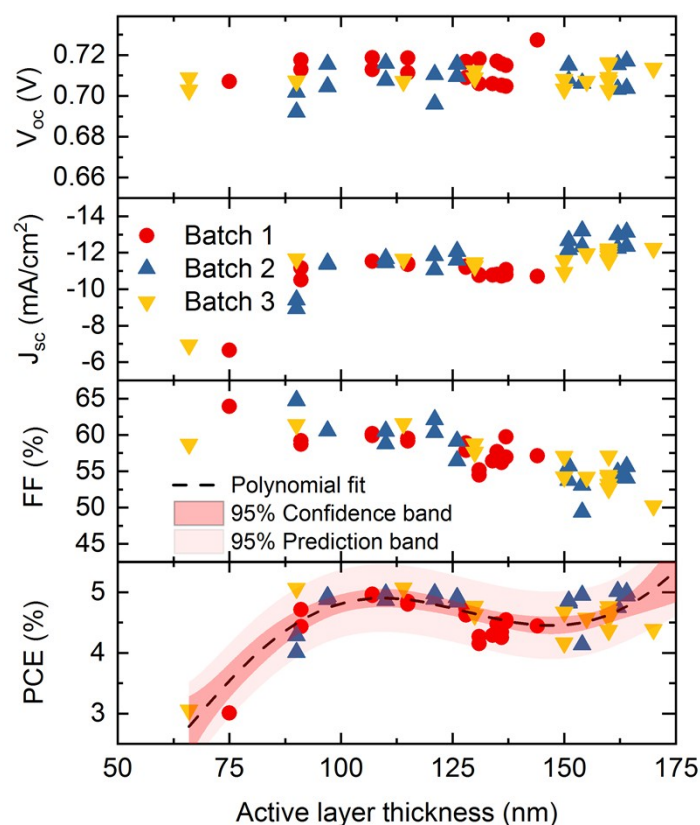


Fig. S5 Reproducibility of doctor-bladed devices with a thickness gradient. Photovoltaic parameters (V_{oc} , J_{sc} , FF and PCE) of devices from three different batches with photoactive layer thickness gradient. The photoactive layer system is P3HT:O-IDTBR.

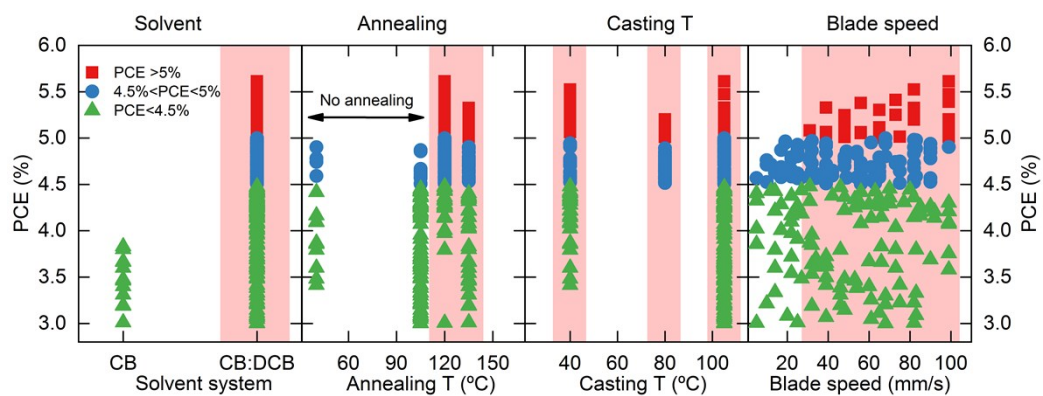


Fig. S6 Multiparametric processing study of the P3HT:O-IDTBR based devices from the database (3% PCE threshold was set). Solvent system, annealing temperature, casting temperature and blade speed (from left to right) as function of PCE. Plot symbols are shape-PCE dependent (red square over 5%, blue circle from 4.5 to 5% and green triangle below 4.5%)

	F (all data)	F >5%	$\Delta\text{PCE}_{\text{max-min}}$ (%)
Acceptor	129	-	4.0
Solvent	84	-	1.7
Annealing temperature	64	1.5	0.6
Casting temperature	40	3.1	0.3
Blade speed	4.3	1.0	0.5

Table S1. Summary of the F parameter of the different processing parameter extracted by analysis of the one-way of variance (ANOVA) for all devices and for those larger than 5%PCE.

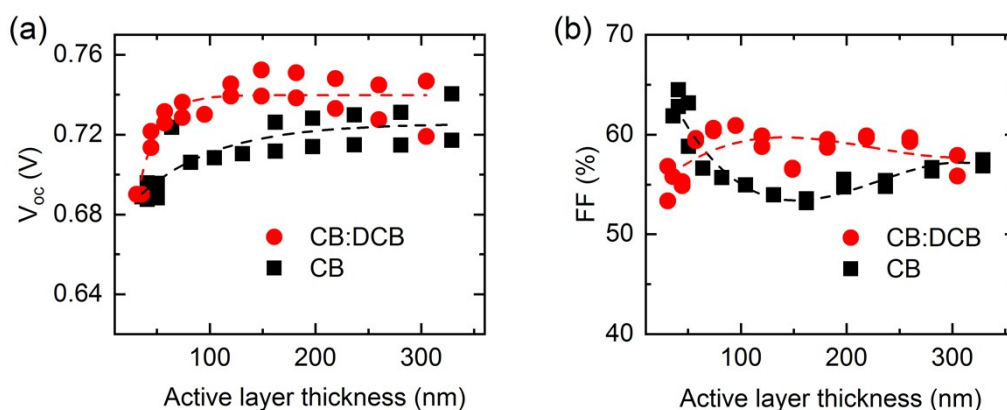


Fig. S7 Photovoltaic parameters of P3HT:O-IDTBR solar cells processed from CB and CB:DCB. (a) Open-circuit voltage and (b) Fill factor. Dashed lines are plotted as a guide to the eye.

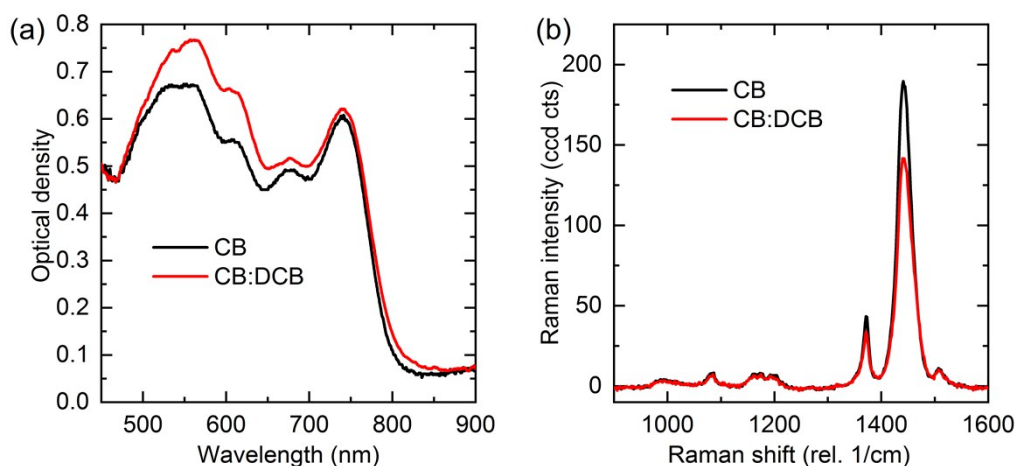


Fig. S8 Optical characterization of P3HT:O-IDTBR devices processed from CB and CB:DCB (1:1). (a) Optical density and (b) Raman shift excited at 488 nm.

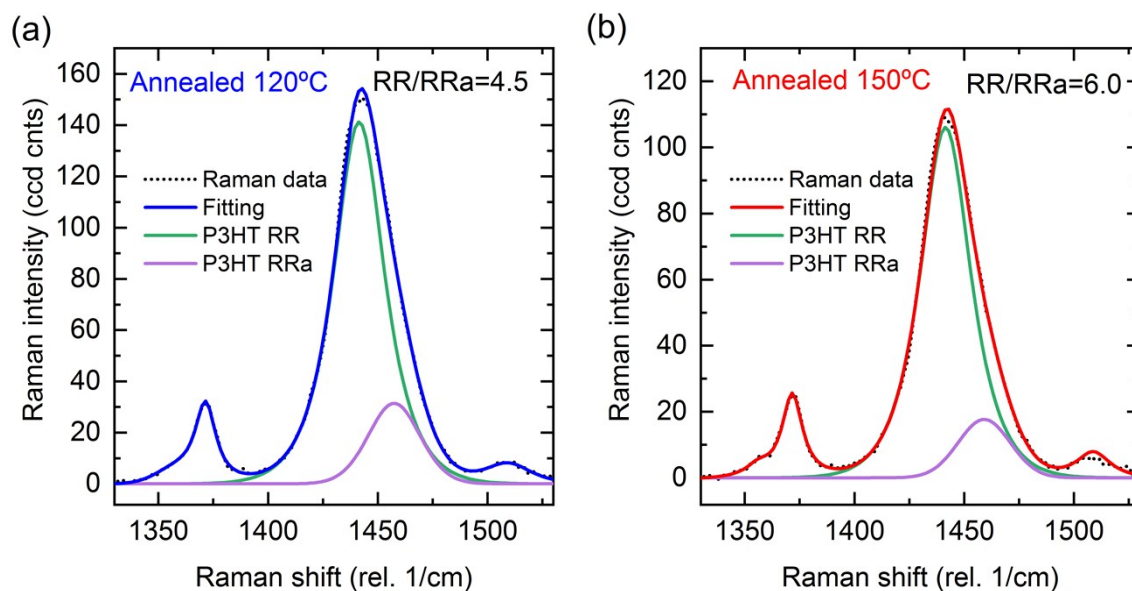


Fig. S9 Example of fitting peaks of Raman spectra excited at 488 nm (**Fig. 5d**) of P3HT:O-IDTBR films for films processed from CB:DCB and (a) annealed at 120°C and (b) 150°C. P3HT regio-regular (RR) and regio-random (RRa) C-C symmetric stretching components are shown in this graph following the method reported in literature [40]. The ratio between RR/RRa is calculated dividing the height of the peaks.

Figure	Ann. T ^a [°C]	Solvent	P3HT Regio Regular peak (RR)			P3HT Regio Random peak (RRa)			RR/RRa (height)
			Center (cm ⁻¹)	Height	FWHM (cm ⁻¹)	Center (cm ⁻¹)	Height	FWHM (cm ⁻¹)	
Fig. S4	As cast	CB	1441.5	182.9	13.5	1458.8	32.8	14.1	5.6
Fig. S4	As cast	CB:DCB	1441.5	137.1	14.3	1460.8	33.5	14.0	4.1
Fig. 5d	120	CB:DCB	1441.5	141.3	13.9	1457.8	31.5	14.3	4.5
Fig. 5d	125	CB:DCB	1441.5	149.6	13.9	1458.4	32.2	14.0	4.6
Fig. 5d	134	CB:DCB	1441.5	149.8	13.9	1458.2	30.0	14.3	5.0
Fig. 5d	140	CB:DCB	1441.5	132.5	13.7	1458.1	25.7	13.7	5.2
Fig. 5d	150	CB:DCB	1441.5	109.1	13.9	1459.1	17.7	13.9	6.0

Table S2 Raman peaks analysis of P3HT:O-IDTBR films from Fig. S4 and Fig. S5. Gaussian Lorentzian crossed function was used to fit Raman spectra. All the Raman spectra were fitted with 6 Lorentzian Cross product peaks and subtracting the background in the same way. All samples were blade cast at 80°C.

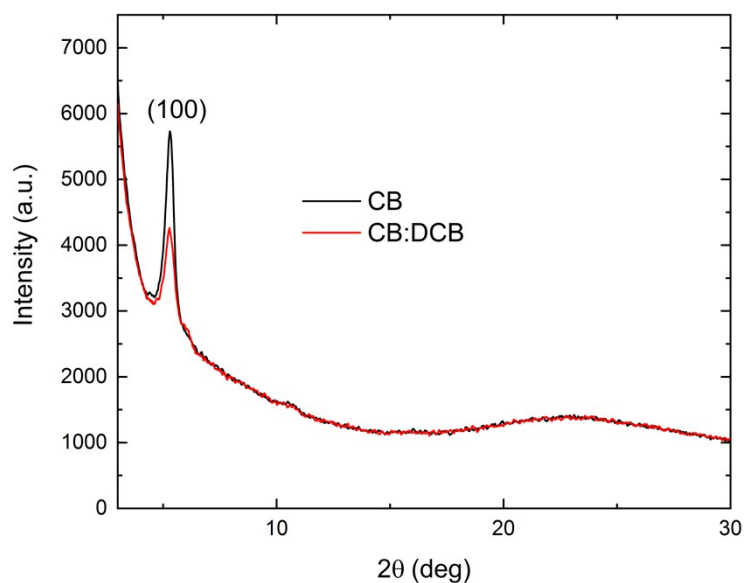


Fig. S10 X-Ray diffraction spectra of the P3HT:O-IDTBR films processed from CB (black) and CB:DCB (red) subjected to post-thermal annealing at 120°C.

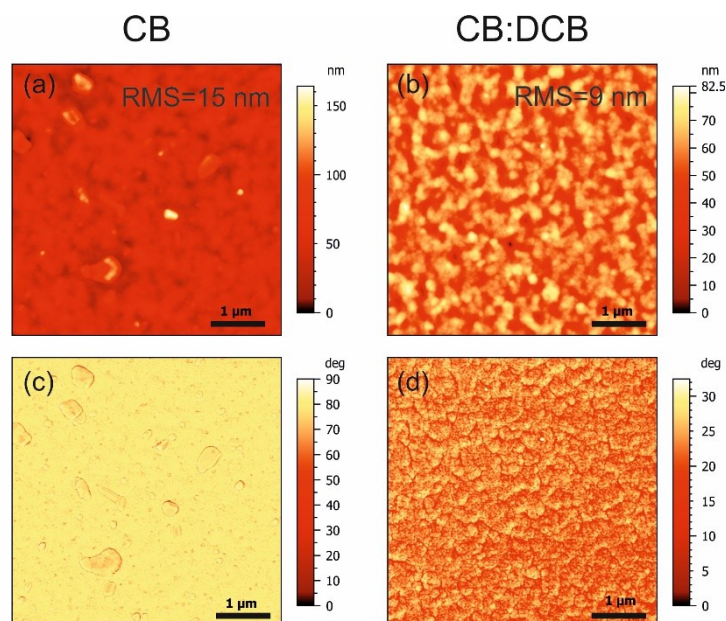


Fig. S11 Surface study upon different solvent system. AFM height (top) and phase (bottom) images of P3HT:O-IDTBR films processed from CB (left) and CB:DCB (right). All AFM image scans are 5 μm x 5 μm.

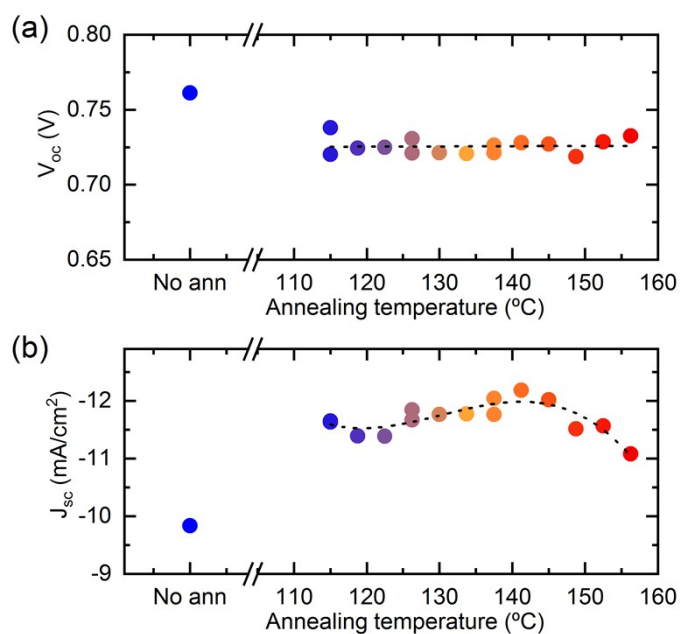


Fig. S12 Annealing gradient effect on photovoltaic parameters of P3HT:O-IDTBR solar cells. (a) Open circuit voltage and (b) Short-circuit current density as function of the annealing temperature. Dashed lines are plotted as a guide to the eye.

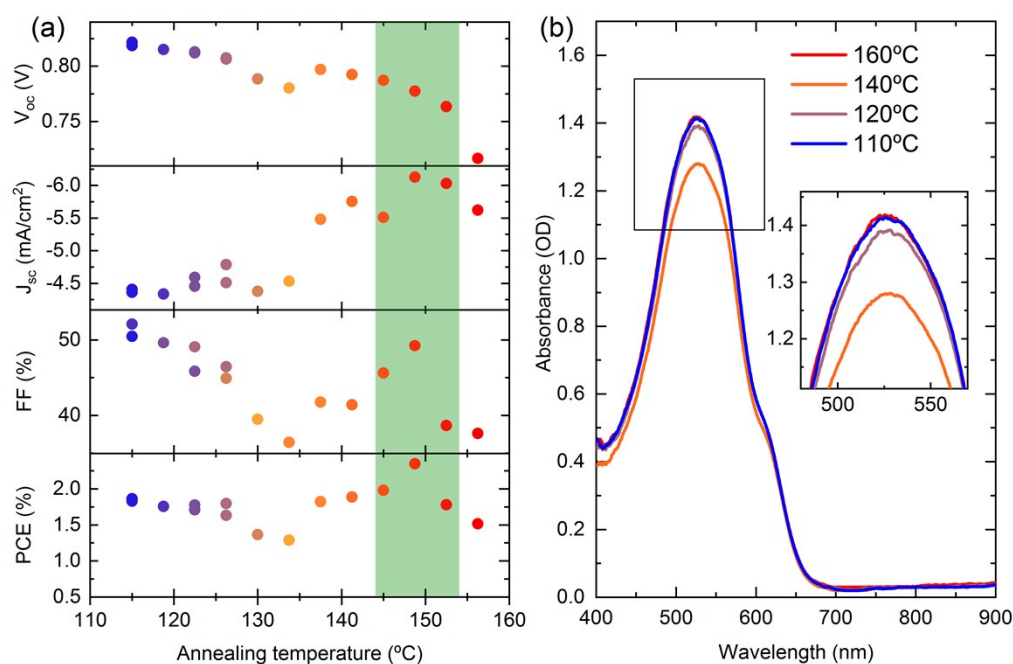


Fig. S13 P3HT:O-IDFBR study upon thermal annealing. (a) Photovoltaic parameters open circuit voltage, short-circuit current density, fill factor and power conversion efficiency. (b) Optical density of annealed samples from 110°C to 160°C. Colours are temperature dependent in plot. Colours go from 110°C (blue) to 160°C (red).

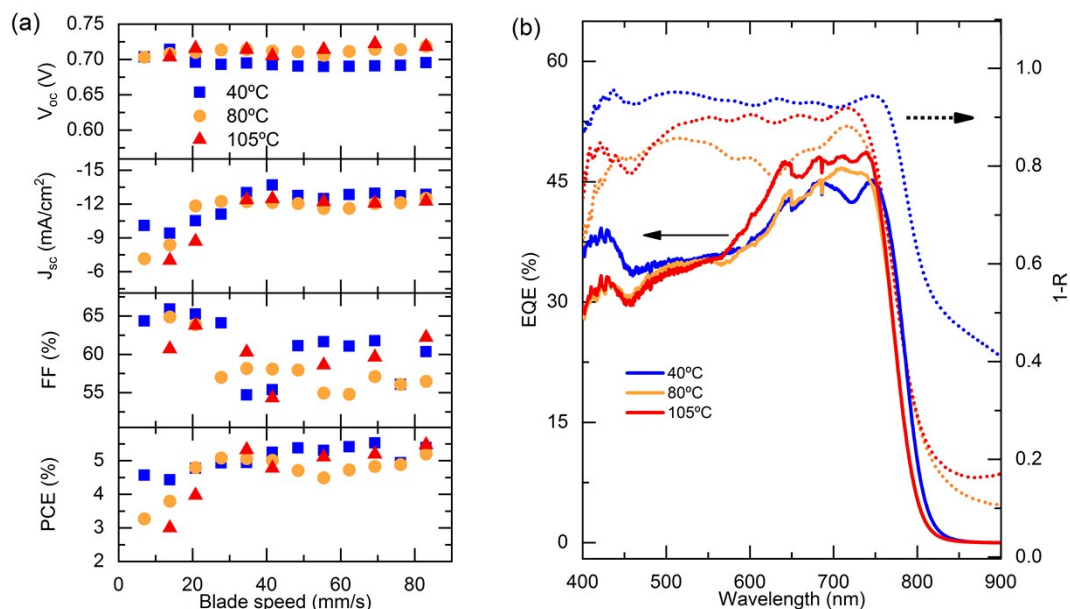


Fig. S14 Casting temperature study for P3HT:O-IDTBR based devices. (a) Photovoltaic parameters such as open-circuit voltage (V_{oc}), short-circuit current density (J_{sc}), fill factor (FF) and power conversion efficiency (PCE). (b) EQE (solid line, left axis) and absorption (1-R) of the full device (dashed line, right axis) are plotted as function of three casting temperatures: 40°C (blue squares), 80°C (orange circles) and 105°C (red triangles).

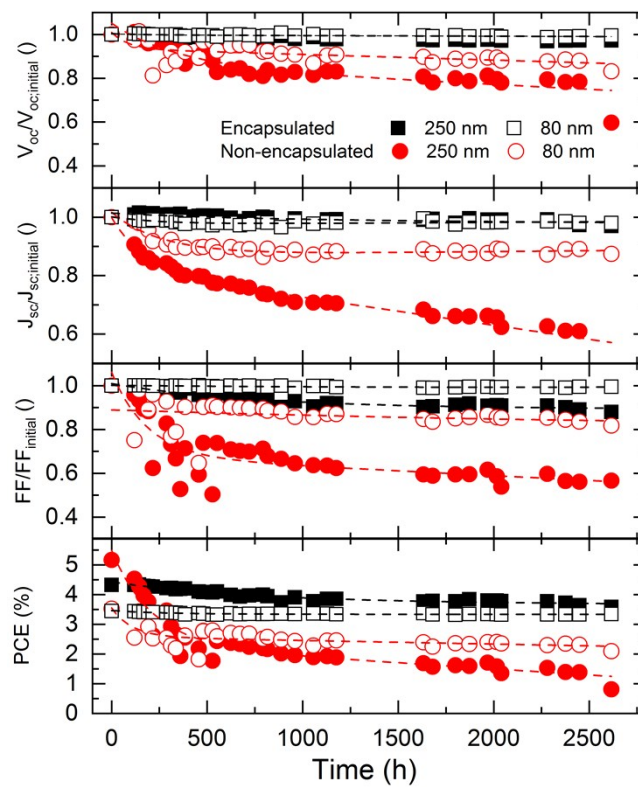


Fig. S15 Photoactive layer thickness and encapsulation effect. Comparison of the photovoltaic parameters (normalized V_{oc} , FF and J_{sc} and absolute PCE) shown in Fig. 6. Dashed lines are plotted as a guide to the eye.

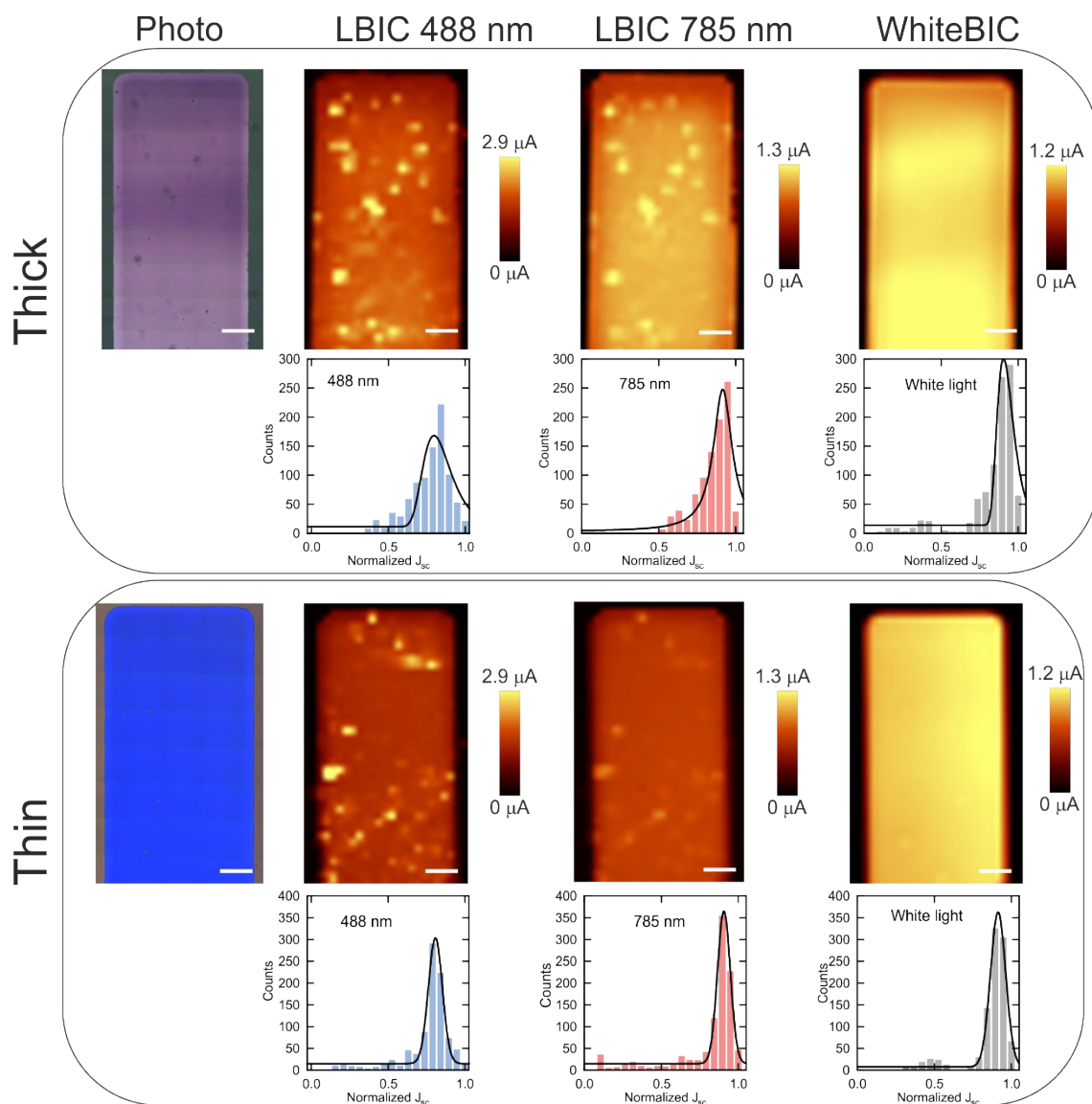


Fig. S16 Comparison of photocurrent maps between thick (top) and thin (bottom) encapsulated films of P3HT:O-IDTBR. Device photo (first column), photocurrent map excited at 488 nm (second column), 785 nm (third column) and with white light (forth column). Normalized statistical histogram is under each photocurrent map. Scale bar correspond to 400 μm in all graphs.

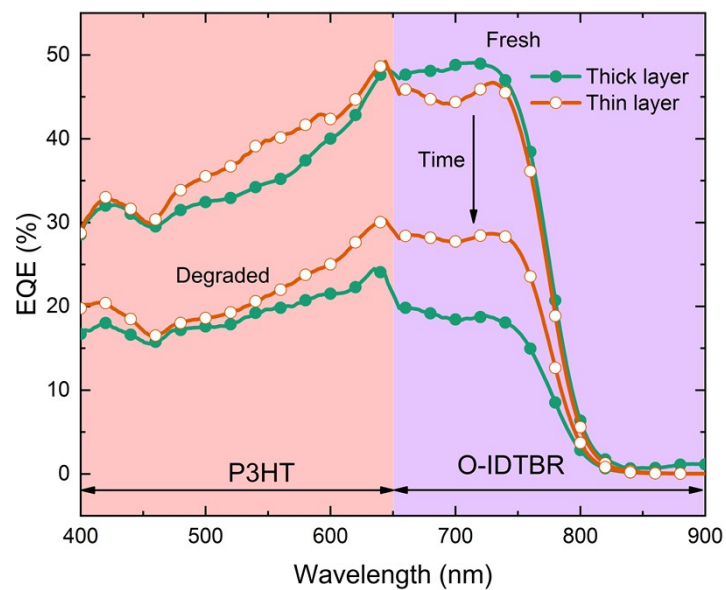


Fig. S17 EQE of fresh and aged P3HT:O-IDTBR non-encapsulated devices as function of the film thickness of the device: thick (filled circle) and thin (empty circle). The arrows of the bottom part represent the main absorption contribution of P3HT (400-650 nm) and O-IDTBR (650-800 nm).